Wavelength-Dependent Differential Interference Contrast Microscopy: Multiplexing Detection Using Nonfluorescent Nanoparticles

ARTICLE *in* ANALYTICAL CHEMISTRY · AUGUST 2010

Impact Factor: 5.64 · DOI: 10.1021/ac101336d · Source: PubMed

5 AUTHORS, INCLUDING:

Yong Luo
Dalian University of Technology
27 PUBLICATIONS **425** CITATIONS
SEE PROFILE

Wei Sun
Washington University
41 PUBLICATIONS **644** CITATIONS
SEE PROFILE

Yan Gu
Harvard University
12 PUBLICATIONS **162** CITATIONS
SEE PROFILE

Gufeng Wang
North Carolina State University
53 PUBLICATIONS **1,206** CITATIONS
SEE PROFILE

Anal. Chem. **2010,** *82,* 6675–6679

Wavelength-Dependent Differential Interference Contrast Microscopy: Multiplexing Detection Using Nonfluorescent Nanoparticles

Yong Luo, Wei Sun, Yan Gu, Gufeng Wang, and Ning Fang*

Ames Laboratory—United States Department of Energy and Department of Chemistry, Iowa State University, Ames, Iowa 50011

The wavelength dependence of plasmonic nanoparticles' contrasts in differential interference contrast (DIC) microscopy has been exploited previously for unambiguous identification and dynamic tracking of these nanoprobes in complex environments (*Anal. Chem.* 2009, *81*, 9203–9208). In the present study, the suitability of multiplexing detection in DIC microscopy was investigated systematically with 19 kinds of nanoparticles of different materials and/or sizes. A unique DIC contrast spectrum was found for each kind of nanoparticle. Multiplexing detection was accomplished by measuring DIC contrasts at a minimum of two specific illumination wavelengths. The main advantages of DIC microscopy for multiplexing detection over other nonfluorescence techniques, such as dark field microscopy and surface-enhanced Raman scattering, were demonstrated by differentiating four kinds of nanoparticles on the cell membrane while providing high-contrast images of both the nanoprobes and cell features.

Multianalyte detection is desirable when developing biomedical and environmental assays. In particular, a number of multiplexing detection schemes based on spectroscopic analysis have been reported.[1−4] The most commonly used scheme employs organic dyes for fluorescence-based detection, which has proved its power in gene sequencing.[5,6] Luminescent quantum dots have been shown to be an excellent alternative to organic dyes for long-term multicolor imaging of live cells.[7] Raman spectroscopy is another suitable tool thanks to the narrow bandwidths of Raman fingerprints.[8−13]

Nonfluorescent nanoparticles have emerged with increasing importance as nonbleaching probes for a variety of optical microscopies.[14] In dark-field microscopy, the Rayleigh scattering of light by nanoparticles results in bright spots over a dark background. Dark-field microscopy-based multiplex identification of biomarkers was demonstrated by Yu et al. using gold nanorods of three different aspect ratios[15] and by Hu et al. using silver nanospheres and gold nanorods.[16]

Differential interference contrast (DIC) microscopy, which generates image contrasts for optical path length gradients in the sample, has been shown to have several advantages over other optical techniques in nanoparticle imaging. DIC microscopy allows the use of full objective and condenser apertures, thus providing the user with the highest lateral resolution and the shallowest depth of field. It also enables simultaneous imaging of nanoparticles and the cellular environment, eliminating the need of switching microscopy modes to correlate the probes and cell features.[17] Recently, we showed that single gold and silver nanoparticles can be selectively imaged in DIC microscopy by varying the illumination wavelength.[18] The dependence of the nanoparticles' DIC contrasts on the illumination wavelength, material, size, and shape implies a new multiplexing detection scheme featuring DIC microscopy.

In this study, we systematically investigated 19 types of nanoparticles: gold nanoparticles of 6 sizes, silver nanoparticles

* To whom correspondence should be addressed. E-mail: nfang@iastate.edu. Phone: (515) 294-1127. Fax: (515) 294-0105.

(1) Bake, K. D.; Walt, D. R. *Annu. Rev. Anal. Chem.* **2008**, *1*, 515–547.
(2) Kunimura, S.; Kawai, J. *Anal. Chem.* **2007**, *79*, 2593–2595.
(3) Phillips, T. E., Bargeron, C. B., Benson, R. C., Carlson, M. A., Fraser, A. B., Groopman, J. D., Ko, H. W., Strickland, P. T., Velky, J. T. In *In-Vitro Diagnostic Instrumentation*; Cohn, G. E., Ed.; SPIE—The International Society for Optical Engineering: Bellingham, WA, 2000; pp 186−192.
(4) Cullum, B. M.; Mobley, J.; Chi, Z. H.; Stokes, D. L.; Miller, G. H.; Vo-Dinh, T. *Rev. Sci. Instrum.* **2000**, *71*, 1602–1607.
(5) Ju, J. Y.; Kim, D. H.; Bi, L. R.; Meng, Q. L.; Bai, X. P.; Li, Z. M.; Li, X. X.; Marma, M. S.; Shi, S.; Wu, J.; Edwards, J. R.; Romu, A.; Turro, N. J. *Proc. Natl. Acad. Sci. U.S.A.* **2006**, *103*, 19635–19640.
(6) Lewis, E. K.; Haaland, W. C.; Nguyen, F.; Heller, D. A.; Allen, M. J.; MacGregor, R. R.; Berger, C. S.; Willingham, B.; Burns, L. A.; Scott, G. B. I.; Kittrell, C.; Johnson, B. R.; Curl, R. F.; Metzker, M. L. *Proc. Natl. Acad. Sci. U.S.A.* **2005**, *102*, 5346–5351.
(7) Jaiswal, J. K.; Mattoussi, H.; Mauro, J. M.; Simon, S. M. *Nat. Biotechnol.* **2003**, *21*, 47–51.
(8) Kalasinsky, K. S.; Hadfield, T.; Shea, A. A.; Kalasinsky, V. F.; Nelson, M. P.; Neiss, J.; Drauch, A. J.; Vanni, G. S.; Treado, P. J. *Anal. Chem.* **2007**, *79*, 2658–2673.
(9) Shah, N. C.; Lyandres, O.; Walsh, J. T.; Glucksberg, M. R.; Van Duyne, R. P. *Anal. Chem.* **2007**, *79*, 6927–6932.
(10) Zavaleta, C. L.; Smith, B. R.; Walton, I.; Doering, W.; Davis, G.; Shojaei, B.; Natan, M. J.; Gambhir, S. S. *Proc. Natl. Acad. Sci. U.S.A.* **2009**, *106*, 13511–13516.
(11) Sun, L.; Yu, C. X.; Irudayaraj, J. *Anal. Chem.* **2007**, *79*, 3981–3988.
(12) Wang, G. F.; Park, H. Y.; Lipert, R. J. *Anal. Chem.* **2009**, *81*, 9643–9650.
(13) Faulds, K.; McKenzie, F.; Smith, W. E.; Graham, D. *Angew. Chem., Int. Ed.* **2007**, *46*, 1829–1831.
(14) Wang, G. F.; Stender, A. S.; Sun, W.; Fang, N. *Analyst* **2010**, *135*, 215–221.
(15) Yu, C. X.; Nakshatri, H.; Irudayaraj, J. *Nano Lett.* **2007**, *7*, 2300–2306.
(16) Hu, R.; Yong, K. T.; Roy, I.; Ding, H.; He, S.; Prasad, P. N. *J. Phys. Chem. C* **2009**, *113*, 2676–2684.
(17) Tkachenko, A. G.; Xie, H.; Liu, Y. L.; Coleman, D.; Ryan, J.; Glomm, W. R.; Shipton, M. K.; Franzen, S.; Feldheim, D. L. *Bioconjugate Chem.* **2004**, *15*, 482–490.
(18) Sun, W.; Wang, G. F.; Fang, N.; Yeung, E. S. *Anal. Chem.* **2009**, *81*, 9203–9208.

10.1021/ac101336d
Published on Web 07/08/2010

of 4 sizes, polystyrene (PS) nanoparticles of 5 sizes, silica nanoparticles of 2 sizes, and poly(methyl methacrylate) (PMMA) nanoparticles of 2 sizes. The DIC images of these nanoparticles were taken at more than 20 illumination wavelengths from 400 to 780 nm, and the DIC contrasts were calculated and plotted in contrast spectra. Each kind of nanoparticle was found to have a unique DIC contrast spectrum, from which we can distinguish it from other kinds of nanoparticles. A practical strategy has also been developed to find the minimum criteria required for identification of a group of selected nanoparticle probes in a real application. As few as two specific wavelengths are adequate in most cases to make confident identification of nanoparticles. We applied the DIC-based multiplexing detection scheme to imaging and identifying four kinds of nanoparticles on the cell membrane simultaneously.

EXPERIMENTAL SECTION

Materials. Silver and citrate-capped gold colloidal solutions were purchased from BBInternational (Cardiff, U.K.) and Nanopartz (Salt Lake City, UT). The PS nanoparticle solutions were obtained from Duke Scientific (Palo Alto, CA). The silica and PMMA nanoparticle solutions were purchased from Bang Laboratories (Fishers, IN). The size distributions were measured by transmission electron microscopy (TEM), and they agreed well with the manufacturer's data.

DIC Microscopy. An upright Nikon Eclipse 80i microscope was used in this study. The DIC mode used a pair of Nomarski prisms, two polarizers, a 100×, 1.40 numerical aperture (NA) Plan Apo oil immersion objective, and a 1.40 NA oil immersion condenser. A Photometrics CoolSnap ES CCD camera (1392 × 1040 imaging array, 6.45 μm × 6.45 μm pixel size) was used to record detailed cell/particle images. A set of 25 filters from Thorlabs (Newton, NJ) have central wavelengths in the range of 400−780 nm and a full width at half-maximum (fwhm) of 10 nm. In addition, a 387 nm band-pass filter (10 nm fwhm) was purchased from Semrock (Rochester, NY). When the DIC microscope was operated at one wavelength, a proper band-pass filter was inserted into the microscope's light path.

Preparation of the Nanoparticle Slides. The DIC contrast spectra of 19 kinds of nanoparticles were acquired by imaging the negatively charged nanoparticles immobilized on the positively charged coverslips. The colloid solutions were first diluted with 18.2 MΩ pure water to proper concentrations and sonicated for 15 min. Then 6 μL of the diluted solution was transferred onto a glass slide and covered with a 22 mm × 22 mm no. 1.5 aminosilane-coated coverslip (Corning, NY).

The DIC contrast spectra of 50 nm gold nanoparticles and 200 nm PS nanoparticles were also acquired when these particles were immersed in air or oil. An aminosilane-coated coverslip was placed on a glass slide with two pieces of the double-sided tape as the spacers to form a chamber under the coverslip. The aqueous nanoparticle solution was loaded into the chamber and adsorbed on the surface of the coverslip. Then the chamber was blown dry by gentle nitrogen gas flow, followed by the acquisition of the DIC contrast spectrum in air. Finally, the microscope immersion oil (refractive index $n = 1.518$; Cargille Laboratories, Cedar Grove, NJ) was added into the chamber, followed by the acquisition of the DIC contrast spectrum in oil.

Preparation of the Cell Slides. The A549 human lung cancer cells (ATCC, Baltimore, MD) were cultured on 22 mm × 22 mm polylysine-coated glass coverslips in a six-well tissue culture plate. The minimum essential cell culture medium (ATCC) with 10% fetal bovine serum supplement was added to the tissue culture plate. The cell culture was incubated at 37 °C under 5% CO_2 until it covered about 70% of the coverslips. A coverslip with cells was rinsed with 1× phosphate-buffered saline (PBS) buffer at pH 7.4 and then placed on a clean glass substrate with two pieces of double-sided tape serving as the spacers to form a chamber under the coverslip. A 10 μL volume of the mixed nanoparticle solution containing 40 and 60 nm gold, 40 nm silver, and 100 nm PS nanoparticles was added into the chamber. The minimum essential cell culture medium was added into the chamber thereafter to prevent the sample from drying out.

Imaging the Sample Slides. For imaging immobilized nanoparticles, the exposure time (0.3−2 s) was adjusted to maintain the same background intensity, and the microscope's focal plane was carefully adjusted to find the highest DIC contrast in all images. Images of nanoparticles adsorbed on the cell membrane were taken under wavelengths of 570 and 440 nm. MATLAB and NIH ImageJ were used to analyze and process the collected images and videos.

RESULTS AND DISCUSSION

Wavelength-Dependent DIC Images of the Nanoparticles. In this attempt to investigate multiplexing detection systematically in DIC microscopy, we took the DIC images of 19 kinds of nanoparticles at a wide range of illumination wavelengths. These images are arranged in a grid (Figure 1) for comparison.

The DIC image size of the same nanoparticle (the images in the same row in Figure 1) generally increases along with the illumination wavelength, while the image sizes of different kinds of nanoparticles at the same illumination wavelength (the images in the same column in Figure 1) remain constant, except for the nanoparticles with diameters greater than 300 nm. These results are expected from the diffraction limit of light, which is defined as the illumination wavelength divided by the sum of the numerical apertures of the objective and the condenser. Nanoparticles with sizes smaller than the diffraction limit have an identical optical image size.

In Figure 1, it is clear that each plasmonic gold or silver nanoparticle reaches a peak DIC contrast at a specific wavelength, while the DIC contrast of other nonplasmonic nanoparticles decreases with an increase of the illumination wavelength. The DIC contrast is defined as the difference between the maximum and the minimum intensities divided by the average local background intensity.

The characteristic wavelength dependency is more evident in the DIC contrast spectra compiled in Figure 2. The PR peaks are observed for gold (Figure 2A) and silver (Figure 2B) nanoparticles, and these peaks are red-shifted as the particle size increases. The DIC contrast of nonplasmonic nanoparticles decreases nearly monotonously with an increase of the illumination wavelength.

Dependence of the DIC Contrast of the Nanoparticles on the Surrounding Medium. The DIC contrast depends on the refractive index difference between the sample and its surrounding

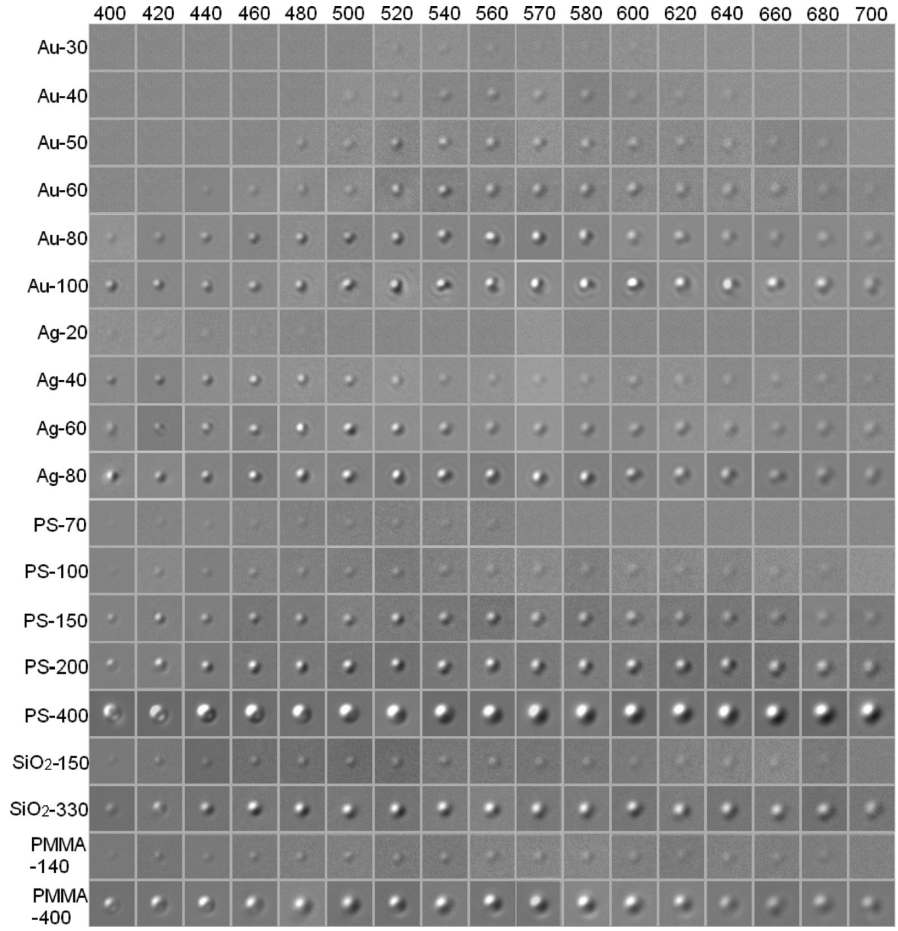

Figure 1. DIC images of 19 kinds of nanoparticles at 17 illumination wavelengths. The images in each row were taken on one selected single nanoparticle. Au-30 means a gold nanoparticle with a diameter of 30 nm and so on for the rest of the notations. All of the images have been adjusted to similar background intensity levels for fair comparison.

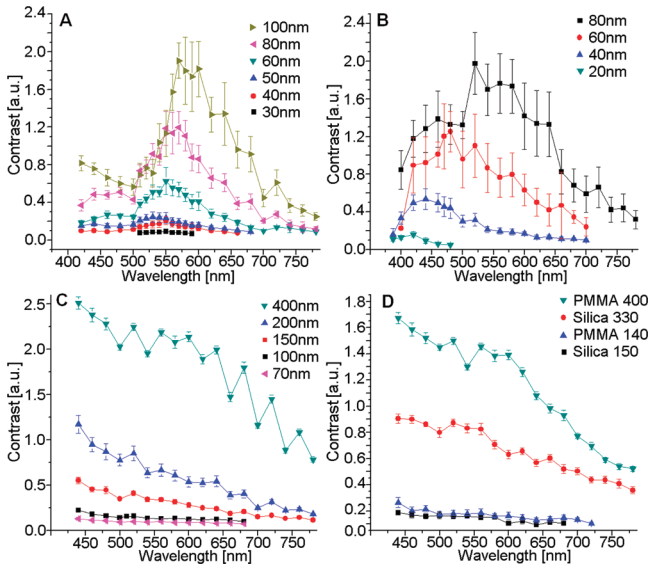

Figure 2. DIC contrast spectra of (A) gold nanoparticles of six sizes, (B) silver nanoparticles of four sizes, (C) PS nanoparticles of five sizes, and (D) silica and PMMA nanoparticles of two sizes each. The DIC contrast of each nanoparticle at each illumination wavelength was calculated by averaging the contrasts of 12 randomly selected nanoparticles. The error bar (1 standard deviation) on each data point reflects the size distribution of this group of nanoparticles.

medium, which in turn causes a phase difference for the two passing beams of orthogonal polarizations. Herein, we selected 200 nm PS and 50 nm gold nanoparticles to investigate the effect of the refractive index difference.

The DIC contrasts of the PS nanoparticles simply increase as the refractive index difference between the particles and the surrounding medium becomes larger, thus showing the highest contrast in air (Figure 3A). The observations for gold nanoparticles are more complex (Figure 3B) because the plasmonic nanoparticle's refractive index varies with the surrounding medium.[19] Unlike the PS nanoparticles, gold nanoparticles immersed in water or oil have higher contrasts than in air, and the PR peaks are red-shifted as the refractive index of the surrounding medium increases from air to water and finally to oil.

Multiplexing Detection Strategy with DIC Microscopy. In principle, different kinds of nanoparticles are distinguishable from one another by comparing their unique DIC contrast spectra. However, collecting spectra is labor-intensive and time-consuming and thus incompatible with high-speed imaging applications. It is essential to find a strategy that minimizes the number of criteria and the amount of time required for confident identification of various nanoparticle probes in complex environments. Herein, we demonstrate that two specific wavelengths are adequate in most cases.

In a DIC multiplexing detection application, a subgroup of the 19 kinds of nanoparticles, as well as other nanoparticles that are not discussed here, should be chosen on the basis of sample

(19) Mock, J. J.; Smith, D. R.; Schultz, S. *Nano Lett.* **2003**, *3*, 485–491.

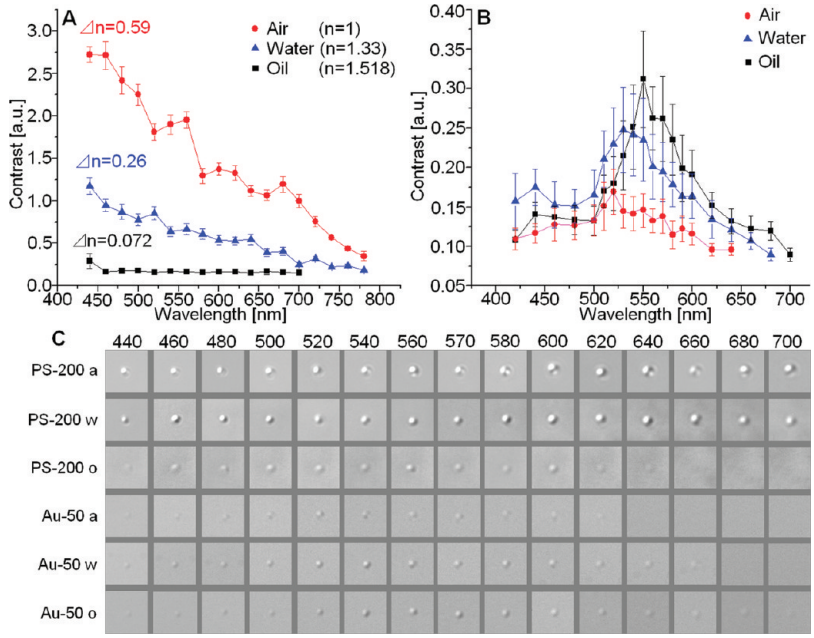

Figure 3. DIC contrast spectra of (A) 200 nm PS nanoparticles and (B) 50 nm gold nanoparticles in air (n = 1.0), water (n = 1.33), and microscope immersion oil (n = 1.518). The sample size for each data point is 12. The refractive index of the PS nanoparticles is 1.59. Δn indicates the refractive index difference between the nanoparticle and the medium. (C) DIC images of a 200 nm PS nanoparticle and a 50 nm gold nanoparticle in air (a), water (w), and oil (o) at multiple illumination wavelengths.

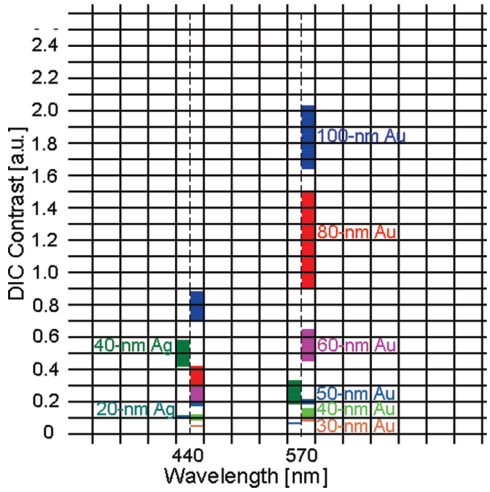

Figure 4. DIC contrast distributions of gold nanoparticles of six sizes and silver nanoparticles of two sizes at wavelengths of 440 and 570 nm. The color bars indicate the full ranges of the measured contrasts.

availability and quality (size distribution, stability, etc.), biocompatibility, and functionalization chemistry. Once selected, the DIC contrast spectra of these nanoprobes are to be analyzed to find the criteria for their identification. An example is provided in Figure 4, in which we show the contrast distributions in grids, instead of the average contrast values as in Figure 2, at two specific wavelengths (440 and 570 nm) for gold nanoparticles of six sizes plus silver nanoparticles of two sizes. The detailed analysis of Figure 4 is as follows: Silver nanoparticles have higher DIC contrast at 440 nm than at 570 nm, while gold nanoparticles have higher DIC contrast at 570 nm. Furthermore, no overlapping of the contrast distributions is found between any two sizes at either wavelength. Thus, gold and silver nanoparticles of different sizes can be readily discriminated. It should be noted that these two wavelengths are not the only combination that leads to confident particle identification. Furthermore, even if the identification of a certain nanoparticle at two wavelengths is not conclusive, an image taken at an additional wavelength is most likely adequate to eliminate any doubt. Similar analysis (Figure S1 of the Supporting Information) is carried out for gold nanoparticles of six sizes plus PS nanoparticles of five sizes. The DIC contrast grid is a convenient and intuitive way of finding the proper wavelengths.

Multiplexing Detection of Nonfluorescent Nanoparticles on Cell Membranes. Visualization of multiple probes on cell surfaces enables detection of multiple biological molecules and related biological processes. In the present study, we demonstrate the simultaneous DIC imaging of four kinds of nanoparticles (40 and 60 nm gold, 40 nm silver, and 100 nm PS nanoparticles) on cell membranes. The preparation of the cell slides is described in the Experimental Section. The DIC images were taken at two wavelengths (440 and 570 nm), and the DIC contrasts were calculated and used to identify the particles. The results of particle identification are shown in Figure 5, and the analysis of DIC contrasts of these nanoparticles is presented in Figure S2 of the Supporting Information. We can clearly visualize and locate all four kinds of nanoparticles on the cell membrane, as well as many cell features, such as the abundant vesicles distributed at the periphery of the cell. Unlike gold or silver nanoparticles, endogenous vesicles display a relatively flatter DIC spectrum that allows them to be distinguished from exogenous nanoprobes.

CONCLUSION

For the first time, DIC microscopy is applied to multiplexing detection of nonfluorescent nanoparticles. Nanoparticles of different materials and sizes can be identified on the basis of their DIC contrasts in the full spectral range or at a minimum of two wavelengths. We imaged and identified four kinds of nanoparticles on the membrane of a living cell and demonstrated one of the major advantages of the DIC multiplexing scheme is the ability

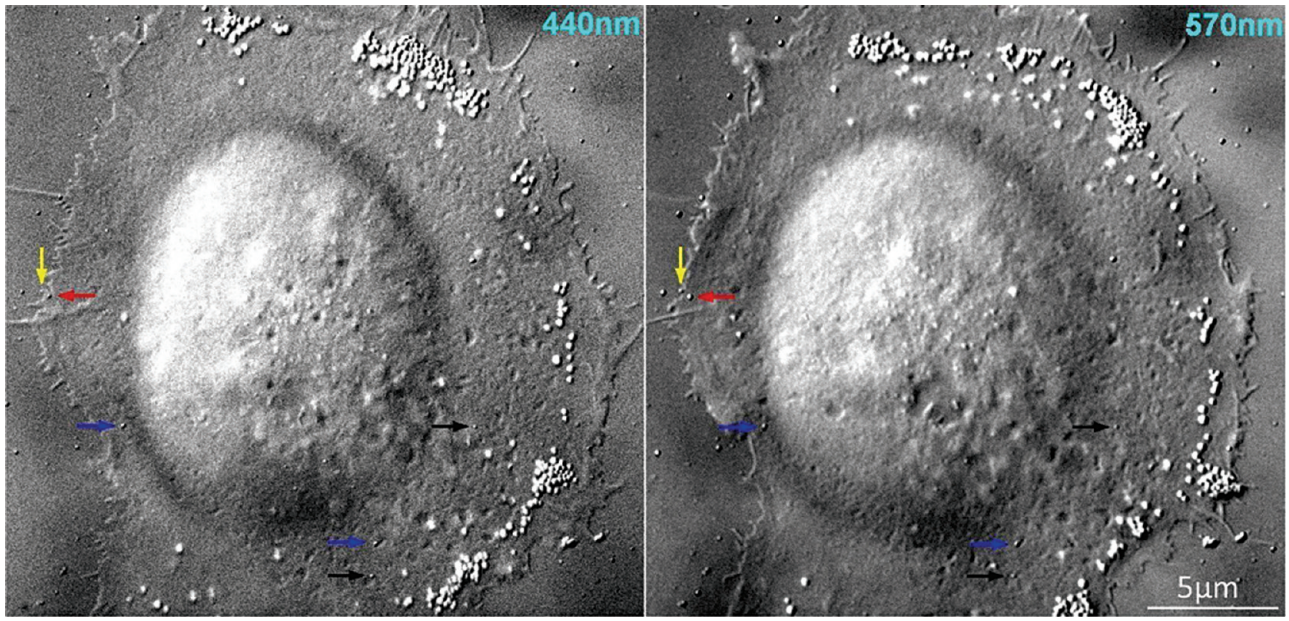

Figure 5. Images of an A549 human lung cancer cell with nanoparticles on its membrane at two wavelengths. Four kinds of nanoparticles are pointed out by yellow (40 nm gold), red (60 nm gold), blue (40 nm silver), and black (100 nm PS) arrows. The morphology of the cell changed slightly because the two images were taken ~2 min apart.

to see both the cell features and nanoprobes with high contrast at the same time. In the cases where two wavelengths are adequate for particle identification, the dual-wavelength DIC microscope that was reported earlier[18] can be employed for real-time imaging of functionalized nanoparticle probes involved in various biological processes on the cell membrane or inside the cell.

ACKNOWLEDGMENT

The Ames Laboratory is operated for the U.S. Department of Energy by Iowa State University under Contract No. DE-AC02-07CH11358. This work was supported by the Director of Science, Office of Basic Energy Sciences, Division of Chemical Sciences.

SUPPORTING INFORMATION AVAILABLE

Additional information as noted in text. This material is available free of charge via the Internet at http://pubs.acs.org.

Received for review May 21, 2010. Accepted June 29, 2010.

AC101336D